Research Square

Preprints are preliminary reports that have not undergone peer review.
They should not be considered conclusive, used to inform clinical practice,
or referenced by the media as validated information.

Smartphone-based Wayfinding Training Improves Spatial Navigation and Reveals Learning Trajectories Associated with ADRD Biomarkers

Jonas Marquardt

jonas.marquardt@dzne.de

German Center for Neurodegenerative Diseases

Niklas Vockert

German Center for Neurodegenerative Diseases

Niklas Behrenbruch

German Center for Neurodegenerative Diseases

Beate Schumann-Werner

Otto-von-Guericke University Magdeburg

Anne Hochkeppler

Otto-von-Guericke University Magdeburg

Eóin N. Molloy

Otto-von-Guericke University Magdeburg

Svenja Schwarck

Otto-von-Guericke University Magdeburg

Larissa Fischer

German Center for Neurodegenerative Diseases

Berta Garcia-Garcia

German Center for Neurodegenerative Diseases

Anna-Therese Büchel

German Center for Neurodegenerative Diseases

Enise I. Incesoy

Otto-von-Guericke University Magdeburg

Hendrik Mattern

German Center for Neurodegenerative Diseases

Jose Bernal

Otto-von-Guericke University Magdeburg

Andrew W. Stephens

Life Molecular Imaging GmbH

Andreas Schildan

Leipzig University
Henryk Barthel
Leipzig University
Osama Sabri
Leipzig University
Michael Kreissl
Otto-von-Guericke University Magdeburg
Emrah Düzel
Otto-von-Guericke University Magdeburg
Esther Kühn
University of Tübingen
Stefanie Schreiber
German Center for Neurodegenerative Diseases
Anne Maass
German Center for Neurodegenerative Diseases
Nadine Diersch
German Center for Neurodegenerative Diseases

Article

Keywords:

Posted Date: June 4th, 2026

DOI: https://doi.org/10.21203/rs.3.rs-9844268/v1

License: This work is licensed under a Creative Commons Attribution 4.0 International License.
Read Full License

Additional Declarations: Competing interest reported. ND is a full-time employee of neotiv GmbH. ED is Co-founder and Chief Medical Officer of neotiv GmbH. AWS is a full-time employer of Life Molecular Imaging GmbH. The remaining authors declare no competing interests.

Smartphone-based Wayfinding Training Improves Spatial Navigation and Reveals Learning Trajectories Associated with ADRD Biomarkers

Jonas Marquardt (https://orcid.org/0000-0002-4796-0864)*[1], Niklas Vockert (https://orcid.org/0000-0001-5915-2517)[1], Niklas Behrenbruch (https://orcid.org/0009-0002-7947-9220)[1,2], Beate Schumann-Werner (https://orcid.org/0000-0002-3530-5766)[2,1], Anne Hochkeppler[3,1], Eóin N. Molloy (https://orcid.org/0000-0002-7804-2214)[4,1], Svenja Schwarck (https://orcid.org/0000-0003-2024-9236)[2,1], Larissa Fischer (https://orcid.org/0009-0001-9936-2954)[1], Berta Garcia-Garcia (https://orcid.org/0000-0002-8585-6507)[1,4], Anna-Therese Büchel[1], Enise I. Incesoy[2,1], Hendrik Mattern (https://orcid.org/0000-0001-5740-4522)[1,5,6], Jose Bernal (https://orcid.org/0000-0003-3167-5134)[2,7,8,9], Andrew W. Stephens[10], Andreas Schildan (https://orcid.org/0000-0002-9418-3826)[11], Henryk Barthel (https://orcid.org/0000-0002-9322-9167)[11], Osama Sabri (https://orcid.org/0000-0002-6425-3504)[11], Michael Kreissl (https://orcid.org/0000-0001-5905-6015)[4,1], Emrah Düzel (https://orcid.org/0000-0002-0139-5388)[2,1], Esther Kuehn (https://orcid.org/0000-0003-3169-1951)[12,2,13], Stefanie Schreiber (https://orcid.org/0000-0003-4439-4374)[1,5,14], Anne Maass† (https://orcid.org/0000-0002-7889-795X)[1,15], & Nadine Diersch†[1]

1) German Center for Neurodegenerative Diseases, Magdeburg, Germany

2) Institute of Cognitive Neurology and Dementia Research, Otto-von-Guericke University Magdeburg, Magdeburg, Germany,

3) University Clinic for Psychosomatic Medicine and Psychotherapy,Otto-von-Guericke University Magdeburg, Magdeburg, Germany,

4) Division of Nuclear Medicine, Department of Radiology & Nuclear Medicine, Faculty of Medicine, Otto von Guericke University Magdeburg, Magdeburg, Germany,

5) Center for Behavioural Brain Sciences (CBBS), Otto-von-Guericke University Magdeburg, Magdeburg, Germany,

6) Biomedical Magnetic Resonance, Otto-von-Guericke University Magdeburg, Magdeburg, Germany,

7) Department of Artificial Intelligence in Biomedical Engineering (AIBE), Faculty of Engineering, Friedrich-Alexander-Universität Erlangen-Nürnberg (FAU), Erlangen, Germany

8) Faculty of Medicine, Friedrich-Alexander-Universität Erlangen-Nürnberg (FAU), Erlangen, Germany

9) Institute for Neuroscience and Cardiovascular Research, Row Fogo Centre for Research into Ageing and The Brain, Department of Neuroimaging Sciences, The University of Edinburgh, Edinburgh, UK

10) Life Molecular Imaging GmbH, Berlin, Germany,

11) Department of Nuclear Medicine, University of Leipzig, Leipzig, Sachsen, Germany,

12) Hertie Institute for Clinical Brain Research (HIH), Tübingen, Eberhard Karls University Tübingen, Germany,

13) German Center for Neurodegenerative Diseases (DZNE), Tübingen, Germany,

14) Department of Neurology, Otto-von-Guericke University Magdeburg, Magdeburg, Germany,

15) Faculty of Natural Sciences, Otto-von-Guericke University Magdeburg, Magdeburg, Germany

*Corresponding Author: Jonas Marquardt (jonas.marquardt@dzne.de)

†These authors jointly supervised this work.

Words: 8445 **Figures:** 8 **Tables:** 2

Abstract

Spatial navigation deficits emerge early in Alzheimer's disease and related dementias (ADRD), yet their potential as a training target and source of digital biomarkers remains underexplored. We evaluated a smartphone-based, unsupervised wayfinding training in 58 cognitively unimpaired older adults and characterized multi-day learning trajectories derived from digital behavioral readouts in relation to neurobiological risk and reserve markers. Participants completed six training sessions navigating to points-of-interest on a university campus, with continuous GPS and app interaction recording. Compared with walking-only controls, participants improved in a pointing task and map drawing, but not in a visuospatial memory task. Higher MTL tau was associated with reduced improvements in navigation efficiency in individuals with greater hippocampal vessel distance. Higher cerebrovascular dysfunction was linked to attenuated learning on readouts reflecting information-processing demands. These findings demonstrate that real-world digital navigation training improves spatial cognition and multi-day learning trajectories show domain-specific associations with ADRD-related biomarkers.

Introduction

The increasing number of people living with dementia poses a growing global health challenge[1]. However, it is estimated that nearly 45 percent of cases are potentially preventable through timely intervention on modifiable risk factors such as physical and cognitive inactivity[2]. The U.S. POINTER clinical trial recently demonstrated that a large-scale multi-domain lifestyle intervention, combining physical activity, nutritional guidance, cognitive training, socially engaging activities, and regular health coaching, can preserve cognitive function in older adults at-risk for dementia[3]. Nevertheless, the long durations and complexity of such programs require substantial clinical infrastructure and resources when delivered on-site under supervision, and their effectiveness depends on sustained adherence over time. This highlights the need for engaging, remotely deliverable interventions that can be implemented without on-site supervision and integrated into everyday life.

Smartphone-based training interventions offer a means to meet these requirements[4] and during such training, multiple digital readouts can be extracted that capture distinct cognitive processes and track subtle dementia-related changes over time. This is particularly relevant in preclinical stages of Alzheimer's disease and related dementias (ADRD), where conventional neuropsychological assessments often lack sensitivity[5,6]. In line with this, Jutten and colleagues[7] demonstrated that diminished multi-day learning curves derived from repeated digital memory assessments are associated with increased amyloid and tau burden in cognitively unimpaired older adults. This suggests that learning trajectories may capture dynamic adaptation processes and thereby provide a more sensitive window into early ADRD-related changes than single-time-point cognitive assessments, which capture relatively static interindividual differences[8]. This sensitivity of learning dynamics may not be confined to memory, and learning trajectories derived from other cognitive domains may show selective associations with distinct ADRD-related biomarkers.

In this context, real-world behaviors that allow multiple cognitive functions to be assessed and targeted simultaneously are particularly relevant. Spatial navigation fulfills these criteria, as successful navigation requires the learning and recall of spatial representations, perspective taking, action planning and goal-directed behavior, as well as path integration (maintaining orientation and tracking self-motion), engaging both medial temporal lobe (MTL) structures and frontoparietal networks[9]. Spatial navigation training using computer-based tasks and virtual reality (VR) environments has been shown to improve spatial navigation performance in healthy older adults[10], and sustained VR training has been associated with relative preservation of hippocampal volume compared with walking-only controls[11]. In addition, spatial navigation combines memory engagement and physical activity within a single behavior, integrating components that have independently been associated with markers of brain health, including reduced tau accumulation and slower cognitive decline in preclinical Alzheimer's disease (AD)[12]. Navigation tasks further generate continuous quantitative behavioral readouts that can be repeatedly sampled in real-world settings[13], making them well suited for modeling learning trajectories over time and their associations with different ADRD-related neurobiological markers.

Spatial navigation critically depends on the structural and functional integrity of the MTL and is therefore among the earliest cognitive functions affected in AD[9], owing to the MTL's vulnerability to early tau accumulation and cortical thinning[14,15]. This vulnerability may nonetheless be contingent upon structural traits, such as the vascular supply of the MTL, measurable via vessel distance mapping. Vascular proximity has been proposed as a potential brain reserve factor, as greater vessel distance has been linked to poorer cognitive performance in the presence of cerebral small vessel disease[16,17]. A lower vessel distance might promote resilience by supporting perfusion, facilitating neuroplasticity, and meeting regional metabolic demands by ensuring sufficient oxygen and glucose supply during task-related neural activity[18]. At the same time, spatial navigation

depends on domain-specific capabilities, such as executive function and processing speed, both of which become disrupted with higher burdens of cerebrovascular disease, such as white matter hyperintensities (WMH) or MRI-visible perivascular spaces (PVS)[19–22]. Together, these biomarkers capture complementary aspects of neurodegenerative and cerebrovascular pathology that may differentially shape navigation learning trajectories.

Here, we evaluate the effects of a remote, unsupervised mobile wayfinding training implemented in a smartphone application ("ExploreTrain") and characterize learning trajectories derived from digital behavioral readouts in relation to ADRD-related risk and reserve biomarkers in cognitively unimpaired older adults. The "ExploreTrain" app is an adaptation of our previously developed "Explore" app[13], which already proved suitable to distinguish between younger adults, cognitively normal older adults and patients with subjective cognitive decline based on different digital readouts (e.g., wayfinding distance and number of orientation stops) during a real-world wayfinding task. The "ExploreTrain" app extends this one-time assessment by implementing a multi-session training program with gamified feedback for better adherence. The training consisted of six sessions divided into egocentric and allocentric conditions across two predefined areas on the medical campus of the Magdeburg university, Germany (Fig 1A). Egocentric sessions required navigation from a fixed start location to individual points-of-interest (POI) and back, thereby supporting the encoding of landmark locations anchored to a fixed start position. Allocentric sessions involved planning and navigating the optimal route connecting three POIs before returning to the start location. Therefore, allocentric sessions required the integration of spatial relations between POIs independent of one's start position. Across sessions, each trial followed the same general structure (Fig. 1B).

From the GPS data and other app data, we derived several digital readouts capturing distinct components of navigation behavior and modeled individual multi-day learning curves (MDLCs)[7,23].

Training-related changes in spatial cognition were assessed by comparing pre- vs. post-training performance on a VR-based pointing task, a map drawing test, and the visuospatial memory test (VWLT)[24]. This allowed us to validate our digital readouts with established markers of navigation ability and to evaluate transfer effects. To control for the effects of physical activity, a walking-only control group completed an equivalent number of sessions walking comparable distances without engaging in a navigation task.

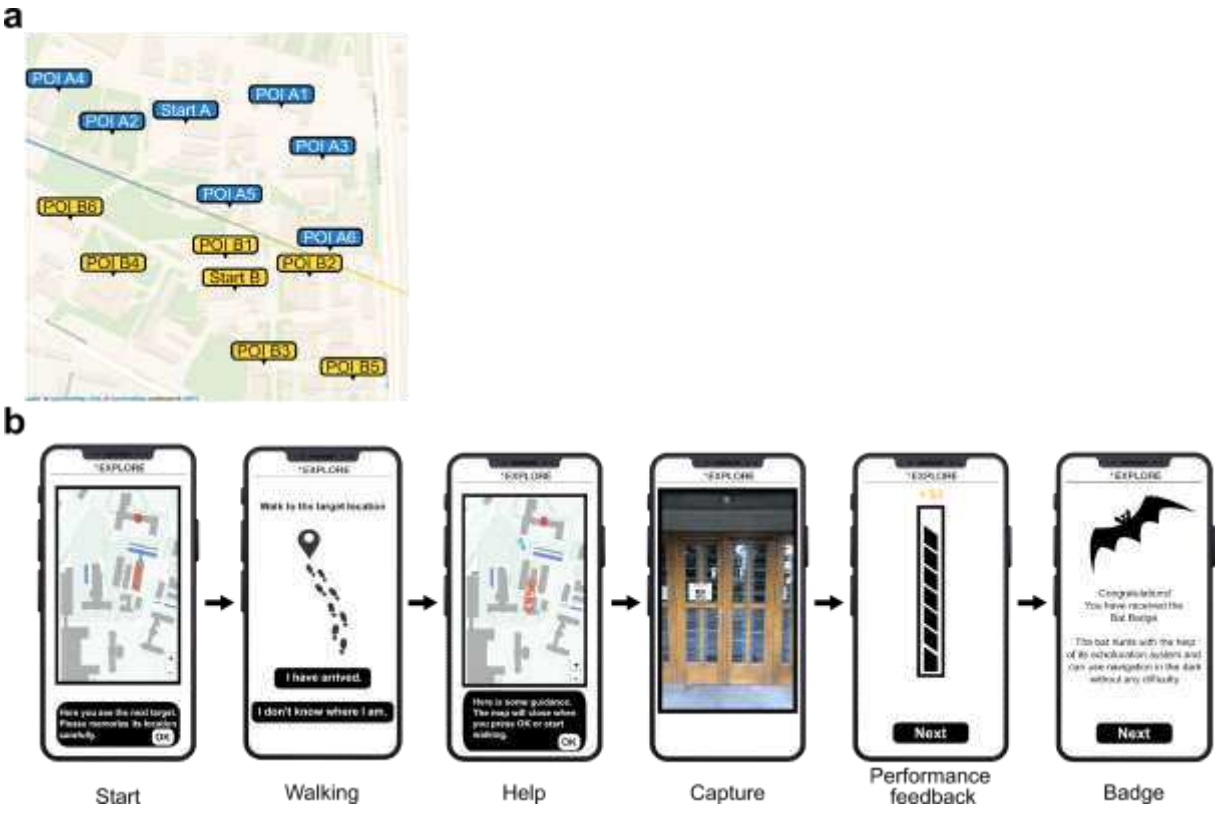


Fig. 1: Wayfinding task implemented in the "ExploreTrain" app. (a) Map of the Magdeburg university campus showing two areas in which the training took place (area A, blue, and area B, yellow). (b) Trial procedure: Participants first viewed a map on the phone showing their current position, the start location of the area they were in and the target POI(s) (start phase). Once they started walking, the map disappeared from the screen (walking phase) and the successful arrival at a POI was confirmed by scanning a QR code (capture phase) before returning to the start location and receiving feedback about their performance (or continuing with the next POI). During walking, participants could view the map again by calling the help function (help phase).

Participants were recruited from a well-characterized research cohort[25] and multimodal neuroimaging was used to assess ADRD-related biomarkers, including MTL tau burden, entorhinal cortex (EC) thickness, hippocampal vessel distance (VD), WMH and PVS. Accordingly, the present study investigates whether distinct learning trajectories during a mobile wayfinding training in the

real world capture domain-specific associations with neurodegenerative and cerebrovascular pathology in cognitively unimpaired older adults. We hypothesized that early MTL tau accumulation would be associated with diminished wayfinding learning trajectories, whereas greater EC thickness and smaller hippocampal VD may buffer against tau-related learning impairments by supporting structural integrity and perfusion. In contrast, higher cerebrovascular dysfunction was expected to preferentially relate to learning trajectories placing greater demands on executive function and processing speed.

Results

Sample characteristics

Sixty-three cognitively unimpaired older adults from the "Human molecular imaging ageing and Superaging" cohort as part of the Collaborative Research Centre 1436 (www.sfb1436.de) were randomized into either the wayfinding training (n = 43) or walking-only control condition (n = 20). Overall, 38 participants (79.16%) successfully completed all six training sessions as well as the post-training assessment, which typically took four to six weeks (median duration = 34 days, range = 18-85 days, see Fig. 2 for the study procedure). The total training time was approximately eight hours per participant. In the control group, all 20 participants completed all sessions. As depicted in Table 1, the two groups did not differ with respect to age ($t(56) = 0.666$, $p = .508$), sex ($\chi^2(1) = 0.076$, $p = .780$), years of education ($t(56) = 0.223$, $p = .823$), familiarity with the environment in which the training took place ($t(56) = 1.323$, $p = .191$), cognitive performance as assessed by the consortium to establish a registry for Alzheimer's disease (CERAD)[26] test battery composite score ($t(56) = -0.605$, $p = .547$), nor MTL tau ($t(45) = 1.508$, $p = .139$).

Table 1. Characteristics of the sample (descriptives, mean scores ± SD)

	Training group	Control group
N	38	20
Age	70.45 ± 5.66	71.45 ± 5.01
No of female (%)	18 (47.4%)	11 (55%)
Years of education	14.76 ± 2.19	14.9 ± 2.29
Environmental familiarity score (range 0 – 1)	0.27 ± 0.18	0.34 ± 0.22

CERAD+ z-value	0.48 ± 0.35	0.42 ± 0.37
	min = -0.25	min = -0.47
Tau PET MTL DVR	0.98 ± 0.05 (n = 29)	1.01 ± 0.06 (n = 15)



Fig. 2: Study procedure. After screening, which consisted of a neuropsychological assessment and multimodal imaging, participants completed a questionnaire assessing familiarity with the environment in which the training took place, a map drawing test, a pointing task in a 3D virtual model of the university campus (during fMRI scanning), as well as the Visual-Way-Learning Test (VWLT)[24]. Participants then completed six sessions of the smartphone-based wayfinding training using the "ExploreTrain" app or an active walking-only control condition. All sessions finished with the map drawing test. Post-training, the VWLT and the VR-based pointing task were performed again. Training participants additionally completed a post-training telephone interview assessing user experience.

Acceptance and usability of the smartphone-based training

Following study completion, participants were contacted via telephone to provide feedback about the training and the usability of the "ExploreTrain" app, as well as their overall user experience (Fig. 3). Most participants agreed or strongly agreed that the app was easy to use (83%), that the instructions were clear (97%) and the duration of the training optimal (92%). The majority found the training engaging (86%) and the cognitive demand appropriate (89%). All participants preferred practicing navigation in a real-world setting over computer-based training and agreed that active health prevention is an important part of their life. 60% of the participants found the possibility to collect points and badges as motivating and 71% also felt that they made progress during the course of the training. However, only 40% could imagine integrating the training into their daily life (and 26% felt neutral about it), even though all of them were fully satisfied with the training in general.

These findings indicate that the "ExploreTrain" app was easy to use and that the training was perceived as engaging and appropriately challenging by study participants. However, further adaptations may be needed to facilitate long-term integration into everyday routines.

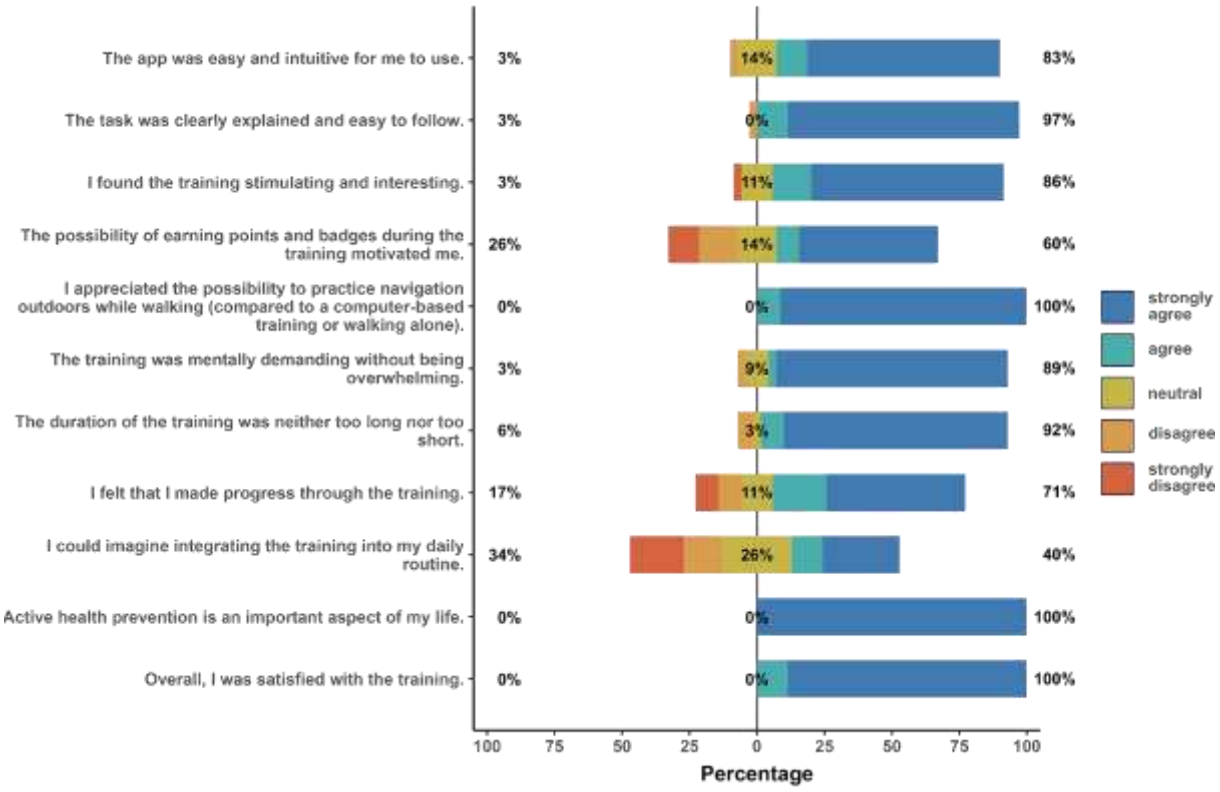


Fig. 3: Acceptance and usability of the training intervention and the "ExploreTrain" app. Results from the telephone interviews after study completion with 35 participants from the training group.

Spatial cognition improved following the smartphone-based wayfinding training

We first compared the performance of the two groups in a pointing task, as a well-established measure for spatial navigation[27–29]. The task was performed in a virtual version of the trained environment, and performance was assessed based on absolute pointing errors before and after training. Using linear mixed-effects models controlling for age, sex, education, and environmental familiarity, we found that the wayfinding training had a positive effect on the pointing accuracy in the VR environment (β = -29.100 [95% CI: -39.370, -18.830], $p < .001$) (Fig. 4A, Supplementary Table 1). While both groups performed slightly below chance level (90°) before the training ($mean_{trainpre}$ = 76.9°, SD = 54.3°; $mean_{controlpre}$ = 70.8°, SD = 51.8°), only the training ($mean_{trainpost}$ = 50.5°,

196 SD = 49.1°) but not the control group ($mean_{controlpost}$= 72.5°, SD = 52.1°) showed a considerable
197 improvement in pointing accuracy after training.

198 Participants in the training group also acquired more landmark knowledge of the trained
199 environment compared with controls as assessed in a pen-and-paper-based map drawing test, which
200 was completed before the training and after each training session (β = 0.096 [95% CI: 0.079, 0.112],
201 p < .00) (Fig. 4C, Supplementary Table 1). Map drawing performance was determined by calculating
202 a metric combining the completeness and correctness of the drawn map, the square root canonical
203 organization (range: 0-1)[30]. Participants in the control group showed an average improvement of
204 0.019 per session, resulting in an overall change of 0.114 from pre- to post-training. In contrast,
205 participants in the training group improved their canonical organization scores by an average of
206 0.115 per session, resulting in an overall improvement of 0.69 from pre- to post-training. This shows
207 that the wayfinding training led to a more accurate cognitive map of the environment.

208 To assess transfer effects on general visuospatial memory, participants additionally
209 completed the pen-and-paper-based VWLT[24]. Across five trials, participants were shown a path of
210 30 interconnected dots among distractor dots and were asked to redraw each path immediately after
211 presentation (immediate recall, maximum score across five learning trials = 150). We did not observe
212 a significant interaction effect of session by group (β = 4.637, [95% CI: -4.435, 13.708], p = .321) (Fig.
213 4B, Supplementary Table 1). Neither the control group ($mean_{controlpre}$= 91.1, SD = 16.7; $mean_{controlpost}$
214 = 93.7, SD = 19.1) nor the training group ($mean_{trainpre}$ = 88.6, SD = 14.1; $mean_{trainpost}$ = 95.9, SD = 20.1)
215 improved their immediate recall performance from pre- to post-training. Thus, no transfer effect of
216 the smartphone-based wayfinding training on general visuospatial memory, as measured in the
217 VWLT, was observed.

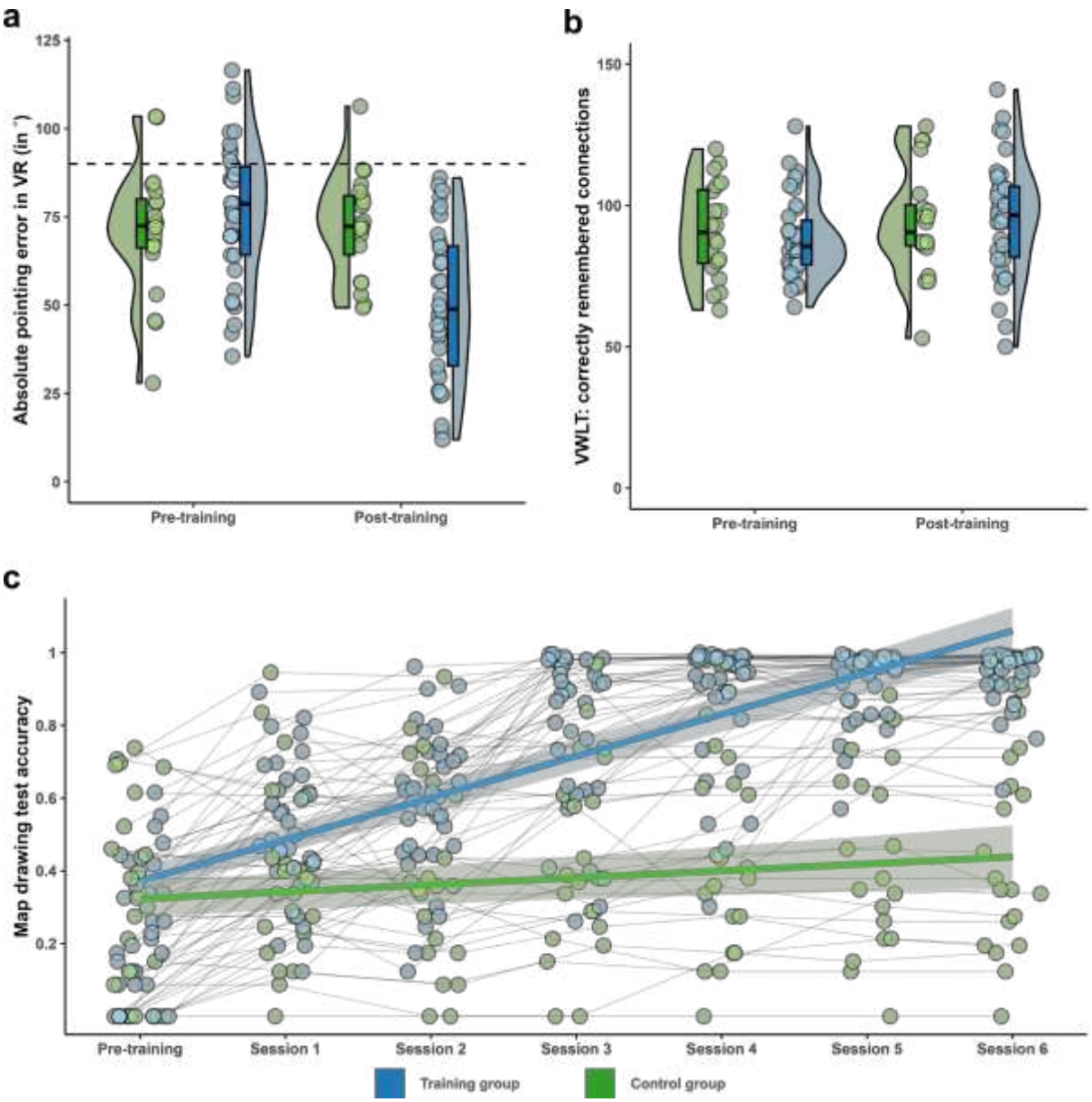


Fig. 4: Performance of the training (blue) vs control group (green) in different spatial cognition tests before and after the training. (a) VR-based pointing task performance shown as absolute pointing error (degrees), with lower values indicating higher accuracy. The dashed line denotes chance level. (b) VWLT[24] performance expressed as the sum of correctly reproduced paths across five learning trials. Boxplots denote the median (center line), interquartile range (box), and 1.5× interquartile range (whiskers) of the measure, dots individual data points. (c) Map drawing accuracy assessed before training and after each training session. The fixed effect of session by group is shown as regression lines with 95% confidence intervals, grey lines denote individual trajectories.

Digital readouts captured training-related improvements in real-world navigation

During the training, the "ExploreTrain" app recorded GPS data and user interactions (e.g., map views) from which five digital readouts were calculated: path deviation (ratio of walking distance to the shortest possible walking distance per track), wayfinding duration, movement speed, number

231 of map views, and number of orientation stops[13]. For each measure, we fitted mixed-effect models
232 with allocentric training session as fixed effect, and random intercepts as well as a random slope per
233 participant, while controlling for the effects of age, sex, and environmental familiarity. Participants
234 showed significant improvements on all five digital readouts (all $p \leq .032$) (Fig. 5, Supplementary
235 Table 2): Across sessions, they took more direct routes, completed the tracks more quickly, and
236 moved at a faster pace. At the same time, they relied less often on the help function and stopped less
237 frequently during walking to orient themselves.

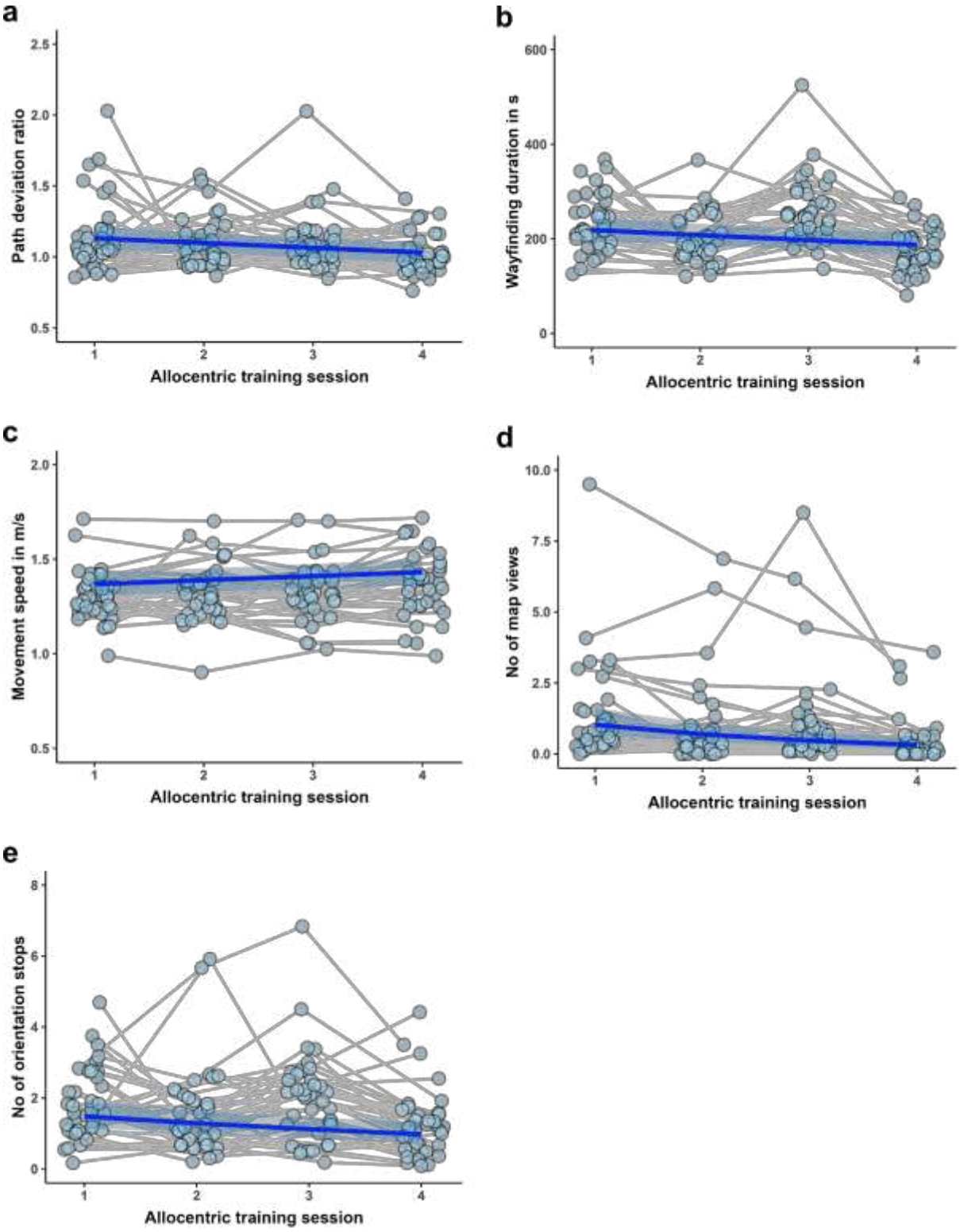


Figure 5. Training-related performance changes in the "ExploreTrain" digital readouts. Mixed-effects model estimates of session effects on (a) path deviation, (b) wayfinding duration, (c) movement speed, (d) number of map views, and (e) number of orientation stops across allocentric training sessions. Blue lines represent model predictions for the allocentric sessions with shaded areas indicating 95% confidence intervals. Grey lines denote individual trajectories and blue dots individual data.

Evidence for three different navigation styles in the training group that were associated with distinct learning trajectories

To identify subgroups of navigators in the training group, a latent profile analysis (LPA)[31] was applied to the data from the egocentric sessions, using the five digital readouts as input features. In egocentric sessions, participants encountered the POIs of the two training areas for the first time, providing a measure of baseline navigation behavior. The LPA identified three distinct navigation profiles that best represented interindividual differences in our sample (Fig. 6): Participants expressing the first profile (n = 15) can be described as "efficient navigators". These participants walked the most direct paths to the POIs, completed the tracks in the shortest time, and walked at a higher speed. They also had a low number of orientation stops and map views, indicating a confident navigation style. The paths of participants in the second profile ("exploratory navigators", n= 12) were the least direct and they required more time to reach the POIs compared with efficient navigators. Their movement speed was lower, and although they relied on the map to a similar extent as efficient navigators, they made more orientation stops. The combination of less direct paths and reduced reliance on app-based support may reflect a more self-directed navigation style. The third profile (n = 11) can be described as "insecure navigators". These individuals walked more direct paths, but required a similar amount of time to complete the tracks and walked slower as the exploratory navigators. They also had a higher number of orientation stops and map views than other participants suggesting a rather cautious navigation style.

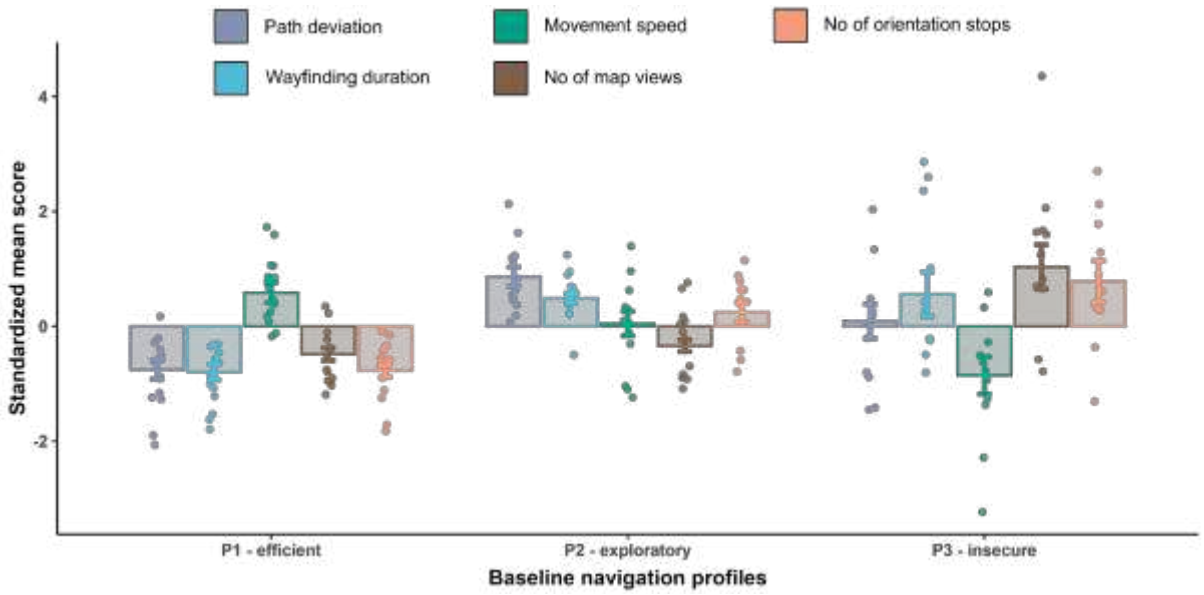


Fig. 6: Baseline navigation profiles in the training group. Average performance (means ± standard error) per digital readout of the efficient, exploratory, and insecure navigators. Dots denote individual data points.

As a next step, we modelled multi-day learning curves (MDLC, i.e., the area under the curve across allocentric sessions, adjusted by performance in the egocentric sessions)[7,23] to quantify individual learning trajectories for each digital readout (see Supplementary Fig. 1 for example MDLC visualizations per readout). When comparing the learning trajectories between the three navigation subgroups, distinct trajectories were observed (Supplementary Fig. 2): Efficient navigators had higher MDLC scores compared with insecure navigators on most digital readouts, including wayfinding duration ($\beta = 0.132$ [95% CI: 0.045, 0.223], $p = .002$), movement speed ($\beta = 0.147$ [95% CI: 0.012, 0.281], $p = .030$), number of map views ($\beta = 0.156$ [95% CI: 0.0533, 0.2579], $p = .002$), and orientation stops ($\beta = 0.154$ [95% CI: 0.070, 0.238], $p < .001$). The MDLC scores for path deviation did not differ significantly ($\beta = 0.129$ [95% CI: -0.007, 0.121], $p = .089$). MDLC scores did not differ significantly between efficient and exploratory navigators for any digital readout (all $\beta \leq 0.036$, all $p \geq .318$). Participants with an exploratory and insecure navigation profile differed in some aspects of learning. While there were no significant MDLC score differences for path deviation and movement speed (all $\beta \leq 0.087$, all $p \geq .302$), exploratory navigators showed significantly higher MDLCs for map views ($\beta = 0.163$ [95% CI: 0.055, 0.270], $p = .002$), and orientation stops ($\beta = 0.102$

[95% CI: 0.0138, 0.191], p = .021), with a trend-level difference emerging for the wayfinding duration MDLC scores (β = 0.093 [95%CI: -0.001, 0.186], p = .052).

These findings indicate that efficient and exploratory navigators exhibited comparable learning trajectories despite using distinct navigation strategies at baseline. In contrast, insecure navigators adapted differently, particularly with respect to their continued reliance on the app's help function and their number of orientation stops, which did not decline over time as in the other two navigation profiles. Having characterized baseline navigation styles and their associated learning trajectories, we next examined whether ADRD-related biomarkers were linked either to baseline navigation profiles or to individual learning dynamics during training.

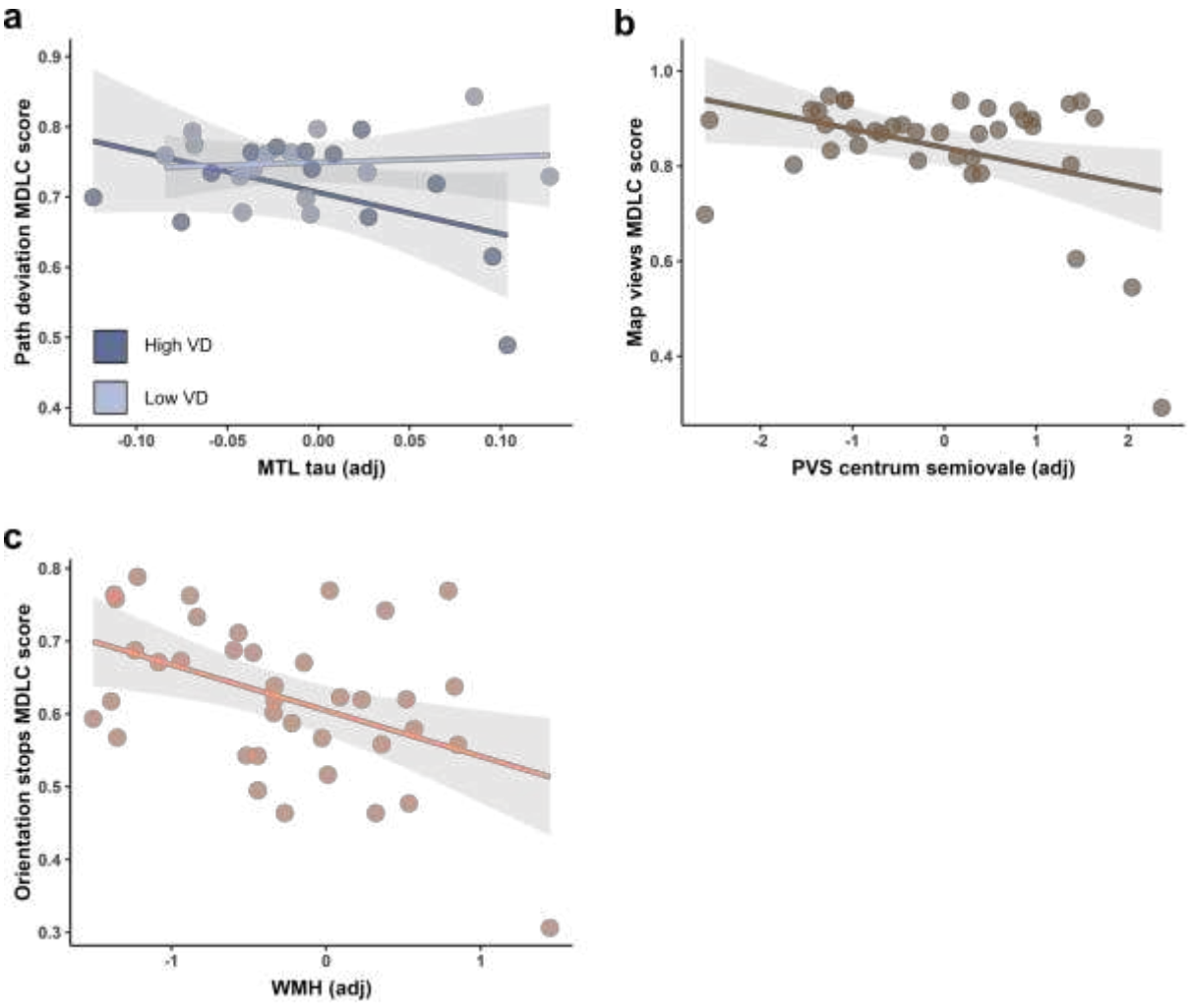
ADRD-related biomarkers did not predict baseline navigation styles

To determine whether there is a link between ADRD-related risk and reserve biomarkers and spatial navigation performance, we first examined whether the three baseline navigation profiles could be predicted by these factors using a multinomial logistic regression model. Neither MTL tau, EC thickness, hippocampal VD, nor one of the cerebrovascular risk factors, centrum semiovale and basal ganglia PVS, or WMH were significantly predicting the baseline navigation profiles of the training group (all $\chi^2(2) \leq 1.809$, all $p \geq .405$). Thus, in this cognitively unimpaired sample, ADRD-related biomarkers were not associated with baseline navigation profiles (Supplementary Table 3).

Higher MTL tau was linked to less efficient path learning in individuals with greater hippocampal vessel distance

Given the crucial role of the MTL in spatial navigation and memory, we examined whether learning-related changes in navigation efficiency, quantified by the path deviation MDLC score, were associated with MTL-specific biomarkers, i.e., MTL tau load, EC thickness, and hippocampal VD. A single linear model was estimated following backward elimination, with path deviation

MDLC score as the outcome and interaction terms between MTL tau load and hippocampal VD, as well as MTL tau load and EC thickness. Although MTL tau was not directly related to the path deviation MDLC score (β = -0.131 [95% CI: -0.606, 0.342], p = .570), we found this relation to be moderated by the hippocampal VD: In individuals with greater hippocampal VD, higher MTL tau was associated with a lower path deviation MDLC score (β = -0.767 [95% CI: -1.532, -0.001], p = .050) (Fig. 7A, Supplementary Table 4). Thus, participants characterized by both elevated MTL tau and greater hippocampal VD showed reduced improvement in path efficiency across sessions. A similar moderation pattern was observed for the relation between MTL tau and EC thickness on the path deviation MDLC score, although this interaction did not reach statistical significance (β = 3.536 [95% CI: -0.359, 7.431], p = .074).



316 **Fig. 7: MDLC scores in relation to ADRD biomarkers in the training group.** Association between (a) MTL tau
317 and path deviation MDLC score, stratified by hippocampal VD (high = dark blue, low = light blue), (b) PVS
318 volume in the centrum semiovale and number of map views MDLC score, (c) WMH volume and number of
319 orientation stops MDLC score. Shaded bands denote the 95% confidence intervals and dots individual data
320 points.

321 **Higher cerebrovascular dysfunction was linked to less learning in digital readouts reflecting reliance**

322 **on the help function of the app and executive control**

323 We hypothesised that cerebrovascular dysfunction would be reflected in MDLC scores for digital
324 readouts placing higher demands on executive function and information processing, namely the
325 number of map views and orientation stops[13]. Consistent with this, individuals with larger PVS in
326 the centrum semiovale continued to rely on the app's help function across sessions (β = –0.039, 95%
327 CI: –0.071 to –0.006, p = .020; Fig. 7B), and those with higher WMH volumes had less pronounced
328 decreases in orientation stops (β = –0.063, 95% CI: –0.106 to –0.020, p = .005; Fig. 7C; Supplementary
329 Tables 5–7).

Discussion

In this study, we show that an unsupervised smartphone-based wayfinding training improves spatial navigation in cognitively unimpaired older adults, with transfer to a pointing task and map drawing. Learning trajectories derived from digital navigation readouts were associated with ADRD-related biomarkers, whereas such associations were not evident when considering interindividual differences in navigation performance at baseline. Specifically, MTL tau and cerebrovascular dysfunction were linked to reduced learning in distinct components of spatial navigation, including interactions between neurodegenerative and vascular markers. Together, these findings show that a multi-day digital navigation training can improve spatial cognition while providing sensitive behavioral readouts of learning processes linked to underlying neurobiological variation in older adults.

In standard neuropsychological assessments, cognitive performance is typically measured at a single time point and impairment is then inferred from deviations relative to normative reference samples[32]. However, in cognitively unimpaired individuals, such assessments may be insensitive to early pathological changes, as compensatory strategies and stable interindividual differences can mask subtle impairments[33]. Previous studies applying digital cognitive assessments across multiple days have shown that diminished practice effects in episodic memory tasks are associated with emerging AD pathology even in the absence of overt impairment[8,14,34,35]. Extending these findings to another cognitive domain, we found in our sample of cognitively unimpaired older adults that navigation styles at baseline did not show detectable associations with ADRD-related biomarkers, whereas multi-day learning trajectories did. This suggests that early neurobiological changes may also manifest as a reduced capacity to improve in specific aspects of real-world navigation. Multi-day learning trajectories derived from digital navigation readouts may therefore provide additional insights into early disease-related changes at preclinical stages[8,36].

In line with this, MTL tau and cerebrovascular dysfunction were differentially related to distinct aspects of navigation learning. Reduced improvements in navigation efficiency were linked to MTL tau burden in individuals with reduced vascular support, consistent with findings on the role of MTL structures in spatial memory and wayfinding[9], as well as with evidence for vascular reserve effects in the MTL[16]. The moderation of tau-related effects by hippocampal VD further supports the notion that local vascular integrity may buffer against early AD-related influences on cognition[37,38]. In contrast, higher cerebrovascular dysfunction, here operationalized as WMH and PVS, was associated with attenuated learning in digital readouts tracking the reliance on the help function of the app and orientation behavior. These behaviors likely place greater demands on executive function and information processing[13], both of which are vulnerable to cerebrovascular pathology as reflected by WMH and PVS[19–21]. This dissociation suggests that digital readouts of the "ExploreTrain" app were able to capture distinct cognitive components supported by separable neural systems that are differentially affected by ADRD-related pathology. This extends prior work on learning trajectories in episodic memory by showing that domain-specific sensitivity to ADRD-related pathology can be resolved within a single, ecologically valid task.

In addition, the mobile wayfinding training was associated with improvements in spatial cognition that extended beyond the trained task. Participants showed better performance in a VR-based pointing task as well as a map drawing test over the course of the training, indicating an enhanced spatial representation of the campus environment. No transfer was observed for the VWLT[24] assessing visuospatial memory, which may reflect limited overlap between the trained navigation processes, such as allocentric representations or spatial updating, and the more sequential and abstract demands of the VWLT. The relatively short training duration may have further limited transfer, as previous studies reporting transfer effects have typically used substantially longer training protocols[11,39]. Nevertheless, the training embedded a cognitively demanding behavior into

an ecologically-valid, real-world context and the unsupervised, smartphone-based implementation enabled a repeated engagement without supervision. Consistent with this, our participants reported a high usability of the app and described the training as interesting and engaging, although only a minority indicated that they could imagine integrating the training into their daily routines. This might have been related to the fixed training environment and the need to travel to the study site. Greater location independence may facilitate integration of the training into everyday life and improve its feasibility. Personalized feedback mechanisms may further support sustained engagement, consistent with evidence that well-designed gamification strategies support long-term adherence[40]. Importantly, the training combined cognitive stimulation with mild physical activity, both of which have been independently linked to brain health and resilience across the lifespan[12,41]. These features position spatial navigation training programs, administered via a smartphone, to complement supervised intervention strategies in decentralized settings.

Spatial navigation is an ability that places concurrent demands on memory, executive function, attention, and motor planning[9], and therefore provides a natural framework for capturing behavior across multiple cognitive domains. The present findings show that, when assessed digitally in a real-world setting, navigation tasks yield continuous behavioral readouts that capture distinct cognitive components and their learning dynamics within a single paradigm. This combination of ecological validity and repeated assessment over time allows behavior to be characterized in a way that more closely reflects everyday function than conventional laboratory-based tasks that target isolated aspects of cognition, while also capturing individual differences in cognitive adaptability that are not reflected in static performance measures obtained at in-clinic visits. Particularly in preclinical stages, where overt impairment is often absent, reduced learning capacity may provide a sensitive signal of emerging pathology[8,36]. Characterizing individual differences in cognitive

adaptability over time may therefore provide a sensitive means to detect early vulnerability and tracking longitudinal change in at-risk populations.

Several limitations should be considered when interpreting our findings. Although the inclusion of an active control group and the repeated multi-day assessments strengthen the interpretability of the observed training effects, the overall sample size was modest, particularly for the tau PET subsample. In addition, our sample consisted of cognitively unimpaired older adults with relatively low pathological burden, which may have limited sensitivity to detect associations between ADRD biomarkers and baseline navigation profiles. Preclinical populations are inherently heterogeneous[42], with individuals following diverse trajectories toward cognitive stability or decline, which further complicates detection of subtle differences in these samples. Replication in larger cohorts encompassing a wider range of biomarker levels will therefore be essential. Another limitation is the relatively short training duration, and the absence of long-term follow-up, which precludes conclusions about the persistence of the training-related improvements or their clinical relevance beyond the immediate post-training assessment. In addition, the real-world aspect of the training introduces variability in participants' experiences. While such variability enhances ecological validity, it may also increase measurement noise relative to controlled laboratory paradigms. Nevertheless, the consistent learning observed across sessions and the selective biomarker associations indicate that meaningful signals were detectable despite this heterogeneity.

Taken together, we show that an unsupervised, smartphone-based wayfinding training is feasible and can improve spatial navigation performance in cognitively unimpaired older adults. At the same time, learning trajectories derived from multi-domain digital navigation readouts collected repeatedly across several days capture aspects of cognitive function that are not reflected in static baseline performance, and show selective sensitivity to ADRD-related biomarkers. Our findings support the use of digital navigation tasks performed in real-world environments as a feasible

425 approach that combines cognitive engagement with physical activity while generating multi-
426 domain behavioral readouts, and thereby complementing the study of early ADRD-related changes
427 in decentralized research settings and lifestyle intervention programs.

Materials and Methods

Participants

All participants were recruited from the "Human molecular imaging aging and SuperAging cohort" as part of the Collaborative Research Centre 1436 (trial registration: https://drks.de/search/en/trial/DRKS00032449; cohort description: https://sfb1436.de/projects/z03-human-molecular-imaging-ageing-and-superaging-cohort/#member-26477-info). This cohort consists of community-dwelling older adults aged 60 years or older who are cognitively unimpaired as assessed via the CERAD-Plus battery[26] according to modified Jak/Bondi criteria[43] (see Behrenbruch, Schwarck and colleagues[25]). For each participant, a CERAD+ composite score was calculated using the age-, sex- and education-corrected z-scores from different sub-tests (Verbal Fluency Animals, Boston Naming Test, Word List Learning Total, Word List Delayed Recall, Word List Recognition, Figures-Copy, Figures-Saving, Verbal Fluency (S-Words), Trail-Making-Test-A, Trail-Making-Test-B)[44]. Additional inclusion criteria were the absence of any psychiatric or neurological condition and major medical illnesses including diabetes, as well as no history of substance abuse or current use of medications that might affect cognition. All participants were smartphone users and therefore familiar with handling mobile devices. Participants underwent multiple MRI sessions during which multi-echo MPRAGE and a fluid-attenuated inversion recovery (FLAIR) sequences were acquired, to derive different cerebrovascular dysfunction measures (see Behrenbruch & Schwarck and colleagues[25]).

A subsample of the participants additionally underwent ultra-high-field MRI scanning on a Siemens Magnetom 7T Plus (n = 57). A high resolution MP2RAGE (0.5mm isotropic resolution, TE = 2.18ms, TR = 4800 ms, TI1 = 900ms, TI2 = 2750ms, flip angle 1 = 5°, and flip angle 2 = 3°) and a time-of-flight angiography sequence (0.28mm isotropic, TE = 4.59 ms, TR = 22 ms, flip angle 19°,

sparse venous suppression[45]), were acquired to visualize hippocampal vasculature by the circle of Willis. A high-resolution turbo-spin-echo (TSE) slab of the MTL was acquired (0.4375 mm x 0.4375 mm x 1.1 mm, TE = 92ms, TR = 8000ms) to segment the hippocampus and subsequently calculate its distance from the surrounding vessels[16]. Overall, the slab was oriented in an oblique-coronal plane, perpendicular to the long axis of the hippocampus and covered a region of 5 cm excluding anterior and posterior parts of the brain. Moreover, 44 participants underwent dynamic [18F]PI-2620 tau-PET imaging using a Siemens Biograph mMR. Approximately 180 MBq (M=182 MBq, std=2.3) was injected intravenously, and structural MRI data were acquired for 60 min in 34 frames (12 x 15 sec, 6 x 30 sec, 4 x 60 sec, 4 x 120 sec, 4 x 180 sec, 2 x 300 sec, 2 x 600 sec).

Procedure

For the purpose of the training, participants were asked to attend a total of eight appointments (Fig. 2), including a pre-training session, six training sessions, and a post-training session. The study was conducted in accordance with the Declaration of Helsinki and was approved by the Ethics Committee of the Otto-von-Guericke University Magdeburg (approval number 193/19). All participants provided written informed consent prior to participation and were compensated for their participation per completed session.

Pre-training assessments

After providing informed written consent, participants first filled an environmental familiarity questionnaire and completed a pen-and-paper-based map drawing task. The environmental familiarity questionnaire, which was adapted from the one used in our previous study[13], consisted of questions about the number and frequency of previous visits on the campus, the number of buildings that were usually visited, as well as the self-rated familiarity with the campus area on a 7-point Likert scale. The questionnaire further consisted of a brief landmark recognition test in which

participants identified familiar buildings from a list of 20 campus landmarks, including POIs from the mobile wayfinding training (Supplementary Fig. 3). A ratio between recognized buildings divided by the total number of buildings was calculated for each participant.

In the map drawing test, participants were presented with a schematic map of the medical campus in which two reference buildings and the main roads were shown (Supplementary Fig. 4). They were asked to indicate the locations of twelve landmarks, which served as POIs in the training, and skip landmarks they did not know. We used the computer-based Gardony Map Drawing Analyzer (GMDA)[30], to assess task accuracy by means of the canonical organization of the filled map. Canonical organization was calculated by performing pairwise comparisons between all possible pairs of landmarks that were marked on the map. The canonical relationships (north/south and east/west comparison) were determined for each pair and a correct canonical comparison received one point. Missing or incorrect landmark comparisons were scored as zero. The square root of the canonical organization score (range 0 - 1) was consequently used as outcome measure with higher scores indicating better configural accuracy and landmark recall. An overall environmental familiarity score was calculated by averaging the landmark recognition score from the questionnaire with the square root of the canonical organization score from the map drawing test. This environmental familiarity score was used as a covariate in our analyses to control for pre-existing interindividual differences in familiarity with the area where the training took place.

As a next step, participants completed a VR-based pointing task (Fig. 8) during a 3T fMRI session (fMRI data will be reported elsewhere). Pointing tasks are an established measure of allocentric spatial knowledge[27–29]. In the present study, the task served as an independent behavioral measure to validate our digital readouts and quantify training-related benefits. The task was performed in a photorealistic 3D virtual environment (VE) developed in Unity (Version 2017.1.17f1, Fig. 8A & 8B), closely resembling the real-world training area. Eight prominent buildings served as

target landmarks in the pointing task, which were also used as POIs in the wayfinding training. The pointing task followed a block design with three navigation blocks and four control blocks in the pre-training assessment (Fig. 8C). Navigation blocks comprised eight trials, whereas control blocks comprised four trials (two in the final block), yielding 24 navigation and 14 control trials in total. Intertrial intervals varied between 1–5 s (mean = 3 s).

Each navigation trial started with a travel phase in which participants were passively transported from a nearby start position towards a reference landmark, covering 15 virtual meters (vm, Fig. 8D). The camera stopped 10 vm in front of the reference landmark (mean travel duration = 4.86 s, SD = 0.11 s). Throughout the trial, an image of a target landmark was displayed at the bottom center of the screen. Once the camera movement stopped, a crosshair appeared on the screen, and participants were asked to indicate the direction of the target landmark relative to their current position by rotating the crosshair (pointing phase) and confirming their response within a 12 s response window. Environmental visibility was limited to a radius of 20 vm by fog and participants were instructed to respond as quickly and accurately as possible. Control trials followed the same structure but required participants to point toward a colored sphere appearing near the stopping location. These trials were included for the fMRI analysis and were not considered in the present study.

Prior to scanning, participants completed a familiarization phase outside the scanner on a desktop PC. During this phase, they were passively transported along a predefined route in the VE (total distance = 1,439 vm, speed = 8 vm/s), encountering all eight target landmarks (see Fig. 8A). In the proximity of each target landmark, the camera stopped moving and turned towards the target landmark for 1 s. Participants also practiced the pointing task in a separate section of the environment. Performance in the pointing task was quantified as the absolute angular pointing error (in degrees) between the indicated direction and the true direction of the target landmark.

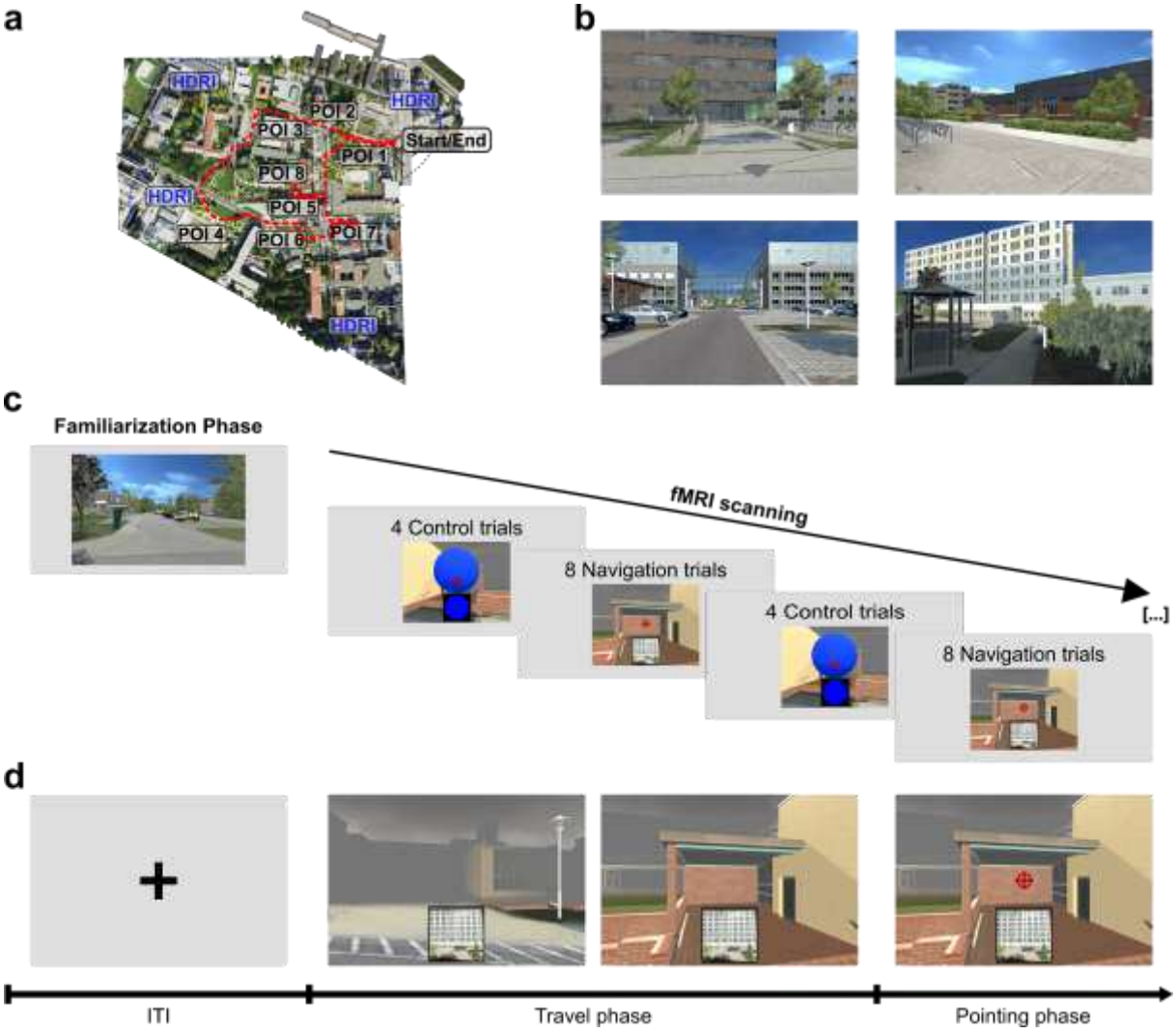


Fig. 8: The VR-based pointing task. (a) Aerial view of the photorealistic 3D model of the medical campus. The red line depicts the route along which participants were passively transported during the familiarization phase. (b) Exemplary point-of-views during the familiarization phase. (c) Block design comprising navigation and control trials. (d) Schematic structure of a navigation trial: passive movement to a reference landmark followed by pointing toward a target landmark.

During the pre-training fMRI session, we also acquired a high-resolution T2-weighted slab covering a region of 12.8 cm, excluding the most anterior and posterior parts of the brain, which was used for hippocampal subfield segmentation. The images were obtained with a voxel size of 0.5 mm × 0.5 mm × 2.0 mm using a TSE sequence (TE = 72 ms, TR = 6000 ms).

As the final step of the pre-training assessment, participants completed the VWLT[24], a standardized pen-and-paper-based measure of visuospatial memory. The test involves learning and recalling one fixed path consisting of 30 interconnected dots embedded among distractor dots. During five consecutive learning trials, the experimenter first shows the path by pointing to each

dot in the correct sequence (encoding). Immediately afterwards, participants are asked to reproduce the entire path on a response sheet (immediate recall). Performance in each trial is scored as the number of correct connections between dots. After these five learning trials, an interference path is presented and recalled once. Participants then reproduce once more the initially learned path, and after a 30-minute delay, both the initially learned and the interference path have to be recalled again (delayed recall). In the present study, analyses focused on visuospatial memory performance during the five immediate recall trials, as the summed immediate recall score represents the primary and most reliable outcome measure for visuospatial memory according to Schellig and colleagues[24].

Training sessions

Participants enrolled in the wayfinding training condition completed a total of six sessions on the medical campus area around the DZNE guided by the "ExploreTrain" app (Fig. 1). At the start of the first session, the experimenter introduced the app and task procedure. Training sessions alternated between two egocentric and four allocentric conditions across two predefined areas of the campus, each with a distinct start location. In egocentric sessions, participants navigated from the start location to one of six POIs and back. These sessions served as an initial encoding phase during which participants learned the locations of POIs relative to a fixed start location. Participants were asked to repeat a path if they deviated from the optimal path by more than 200 m. In allocentric sessions, participants planned and walked the shortest route connecting three POIs from the egocentric sessions, before returning to the start location. In total, four routes were completed covering 12 POIs in total. In each trial (ego- and allocentric), participants first viewed a map on the phone showing their current location, the start location of the area they were in, and a location pin of the target POI(s). A pop-up window showing a photo of the POI could be opened by pressing on the respective location pin. Participants were instructed to close the map before they started walking and to find the POIs independently. Once they started walking (or after 20 s), the map automatically

disappeared from the screen but could be re-opened, if needed. A QR code, which was placed at the entrance door of the POI, had to be scanned with the phone camera once the participant arrived there. This confirmed the completion of the current path and initiated the corresponding procedure for the next path.

We implemented a gamified feedback system in the app, consisting of star ratings, performance points, and badges to sustain participant engagement throughout the training. After each completed trial, participants received one to three stars based on the deviation between their walked distance and a predefined reference distance. Receiving only one star in an egocentric trial triggered the repetition of that trial to ensure proper encoding of the landmark locations. Participants additionally earned points after arriving at each POI, based on their navigation accuracy adjusted by a small penalty for each use of the help function. These points filled a progress bar and when reaching a predefined point threshold, animal-themed badges were unlocked, shown in a pop-up window, that symbolized increasing levels of navigational proficiency. All participants who completed the training also reached the highest level of performance in terms of badges that could be collected.

During training, GPS and meta data (e.g., number of map views) were recorded. From these data, five digital readouts were derived to capture complementary aspects of real-world navigation behavior. Participants enrolled in the control condition completed six sessions during which they were asked to walk comparable distances (~5000 steps) without a navigational component. This took place on the main campus of the Otto-von-Guericke University in Magdeburg, located approximately 4.5 km from the medical campus, and their adherence to the protocol was monitored via a step counter. After each session, participants from both groups completed the map drawing test again to assess changes in landmark knowledge.

Post-training assessments

After the training, all participants completed the VWLT once more, using a parallel version of the task. The study concluded with a second 3T fMRI scan, in which participants again performed the VR-based pointing task, this time consisting of four navigation blocks with 32 trials.

User experience questionnaire

Participants in the training group completed a structured telephone interview after study completion. During the interview, they rated their user experience across eleven statements on a 5-point Likert scale (1 = totally disagree, 5 = totally agree, Fig. 3).

GPS data preprocessing

The GPS data from the training were preprocessed using R (version 4.5.0, R Core Team, 2024). Duplicated entries, recording artifacts, and GPS points within a 15 m radius of each POI, when the QR code sign was visible, were removed. Data from the initial map viewing phase at the beginning of each trial as well as data from the return paths to the start location were also excluded from analyses (see Supplementary Fig. 5 for a visualization of the preprocessed GPS data). A total of 236,782 GPS coordinates, recorded every 2 seconds, from 2193 trials were used in subsequent analyses.

Digital readouts

Five digital readouts were extracted from the app data to capture distinct aspects of real-world navigation performance: path deviation, wayfinding duration, movement speed, number of map views, and number of orientation stops[13]. Path deviation was calculated by dividing the total wayfinding distance, obtained from the haversine distance of consecutive GPS coordinates, by the shortest possible walking distance for each trial, as extracted from OpenStreetMap (https://www.openstreetmap.org/copyright/en) under the Open Database License using the osrm

606 path (https://project-osrm.org/). In this way, the wayfinding distance was normalized by the
607 environmental features of the trials to account for between-session differences in overall distances.
608 Wayfinding duration was calculated by summarizing the timestamps for each trial. Movement speed
609 was calculated by dividing wayfinding distance by wayfinding duration. The number of times
610 participants called the help function during walking was recorded by the "ExploreTrain" app for
611 each trial. We further calculated the number of orientation stops, defined as the number of times a
612 participant spent more than five seconds moving less than a meter while navigating towards a POI[13].

613 **Cerebrovascular dysfunction assessment**

614 Perivascular spaces (PVS), an imaging marker of cerebral small vessel disease, were segmented from
615 the T1-weighted and FLAIR imaging data using a semi-automated pipeline[46,47]. Segmentation took
616 place across two regions of interest (ROI): the basal ganglia (BG) ROI encompassed the caudate
617 nucleus, lentiform nucleus, thalamus, and adjacent internal and external capsules, whereas the
618 centrum semiovale (CSO) ROI included the remaining supratentorial white matter. The delineation
619 of the ROIs follows established visual rating conventions[48]. All PVS segmentations underwent visual
620 inspection and manual correction for false positives. PVS burden was calculated as fractional volume
621 (PVS_volume / ROI_volume) and normalized using the *bestNormalize* algorithm[49] to correct for
622 skewness.

623 White matter hyperintensities (WMH), another imaging marker of cerebral small vessel
624 disease, were segmented from the T1-weighted and FLAIR sequences using the AI-powered Lesion
625 Segmentation Toolbox (LST-AI)[50]. Total and regional WMH volumes (across cortical lobes, corpus
626 callosum, and internal/external capsules) were subsequently extracted using the USCLobes Atlas[51].
627 To address distributional non-normality, WMH volumes were Box-Cox transformed. Total
628 intracranial volume (TIV) correction was performed via linear regression, and the resulting residuals
629 from the TIV-WMH model were used in subsequent analyses.

630 **Hippocampal vessel distance calculation**

631 High-resolution (7T) T2-weighted slab images optimized for medial temporal lobe (MTL) volumetry
632 were segmented using the Automatic Segmentation of Hippocampal Subfields (ASHS) software[52].
633 The ASHS pipeline provides fully automated labeling of hippocampal subfields (including CA1,
634 CA2, CA3, dentate gyrus, and subiculum) as well as cortical subregions of the perirhinal (Brodmann
635 areas 35 and 36), parahippocampal, and entorhinal cortex. The ASHS segmentations were visually
636 inspected, and manual corrections were applied where necessary. In total, 42.4% of hemispheres
637 required correction. Subsequently, cerebral vessels were segmented from time-of-flight (ToF)
638 angiography data using a publicly available pipeline for small vessel segmentation[53]. Vessel maps
639 were visually quality-controlled and coregistered to the corresponding T2-weighted MTL images
640 via an intermediate coregistration to the corresponding T1-weighted image. To quantify regional
641 vascular proximity, VD maps were computed using the previously established method vessel
642 distance mapping[16]. Lastly, to account for individual differences in hippocampal volume, average
643 vessel-to-hippocampus distances were calculated after spatial normalization of the VD maps to MNI
644 space. A generic hippocampus mask that had been obtained by Freesurfer segmentation of the MNI
645 template served as ROI.

646 **MTL tau quantification from PET imaging**

647 All dynamic images acquired in the PET scanning session were corrected for motion and registered
648 to the individual T1-MRI. T1-weighted images were segmented with Freesurfer to derive ROIs. To
649 generate parametric images expressed as distribution volume ratio (DVR), we applied Multilinear
650 Reference Tissue Model[54] in QModeling (version 3, in Matlab Version R2024V). The inferior
651 cerebellum was chosen as low receptor binding region/reference region, and the globus pallidus as

high receptor binding region[54,55]. The MTL ROI, of interest in this study, covered the entorhinal cortex, parahippocampal cortex, amygdala, and fusiform gyrus.

Medial temporal lobe subregional thickness estimation

To determine the surface-based cortical thickness of MTL subregions, T2-weighted images acquired at the pre-training assessment were segmented using ASHS[52]. The resulting segmentations were then processed with the cortical reconstruction for automatic segmentation of hippocampal subfields (CRASHS). CRASHS is a surface-based modeling and groupwise registration framework specifically tailored to MTL subregions. It leverages the ASHS-labeled segmentations and generates a series of surfaces spanning from the gray/white matter boundary to the pial surface. This approach quantifies cortical thickness within MTL subregions, such as the entorhinal cortex, and is sensitive to subtle region-specific effects of aging and neurodegeneration[14].

Statistical analysis

All statistical analyses were performed using R (version 4.5.0., R Core Team, 2024).

Pre- to post-training changes in spatial cognition measures

To investigate the effect of the smartphone-based wayfinding training on performance in the VR-based pointing task, we fitted a linear mixed effect models (LME)[56] on the absolute pointing error data with fixed effects for session, group (training vs. control), and their interaction, as well as covariates for age, sex, years of education, and environmental familiarity. Random intercepts were specified for each trial to account for specific differences in features such as rotation angle, visual similarity between landmarks, or prior exposure to landmarks. We further specified random intercepts for participants, with random slopes for session by participant. Accuracy in the map drawing task was modeled using a LME model with the same specifications, but session treated as a

continuous variable. VWLT performance was analyzed in terms of immediate recall scores with the same fixed effects, a random intercept per participant, and covariates as in the other LMEs, except environmental familiarity.

Modeling training-related changes in digital readouts

Linear and generalized mixed-effects models were used to assess changes in the five digital readouts across allocentric sessions[56,57]. Continuous outcomes (e.g., path deviation, log-transformed wayfinding duration, and movement speed) were modeled using LMEs[56], with fixed effects for session, age, sex, years of education, and environmental familiarity. Random intercepts for path and participant as well as random slopes for each individual were included. For count-based outcomes (number of map views and orientation stops), generalized mixed effect (GME) models with a zero-inflated negative binomial distribution were estimated[57], with analogous fixed and random effects.

Multi-day-learning-curve scores

For each digital readout, multi-day learning curve (MDLC) scores[7,23] were calculated to quantify individual learning trajectories across training sessions by capturing systematic session-level changes in performance beyond trial-level variability. Linear regression models were fitted separately for each digital readout, and standardized residuals were extracted at the trial level after adjusting for age, sex, environmental familiarity and track (where applicable, Supplementary Table 8). These residuals were averaged across trials for the two egocentric sessions to derive a baseline performance estimate, and separately averaged for each of the four allocentric sessions. To ensure comparability across measures, four of the digital readouts (except movement speed) were inverted such that higher values reflected better performance with a minimum value of zero. Individual MDLC scores were computed using an area-under-the curve (AUC) approach summarizing the baseline performance with the learning trajectories over the allocentric sessions, consistent with

prior work[7,23]. To isolate learning from baseline performance differences, raw AUC values were scaled to each participant's baseline performance and to obtain a sample-derived optimal performance. Optimal performance was defined empirically as the best observed performance within the sample for each digital readout in each session. This normalization yielded baseline-adjusted MDLC scores ranging from 0 (no learning) to 1 (learning equivalent to the sample-specific optimum).

Baseline navigation profiles

To identify baseline navigation profiles independent of training effects, analyses were restricted to the two egocentric sessions, in which participants encountered the POIs for the first time. Participants' z-standardized residuals from the linear regression models (Supplementary Table 8) were averaged across the two egocentric sessions and submitted to a latent profile analysis (LPA)[31]. We fitted models with two to five profiles to the data and evaluated them based on multiple fit indices with the constraint that each profile should contain at least 15% of the sample (Table 2). The three-profile model was selected as optimal and used in subsequent analyses.

Table 2: Model fit statistics of the latent profile analysis (LPA)

Model	AIC	BIC	SABIC	Entropy	BLRT p-value	N assigned to each profile
2-Profile	516.789	551.178	485.516	0.856	.010	P1 = 22, P2 = 16
3-Profile	500.855	553.258	453.202	0.909	.020	P1 = 15, P2 = 12, P3 = 11
4-Profile	498.968	569.384	434.933	0.942	.277	P1 = 7, P2 = 6, P3 = 15, P4 = 10
5-Profile	492.197	580.627	411.781	0.939	.059	P1 = 6, P = 5, P3 = 7, P4 = 10, P5 = 10

AIC = Akaike information criterion, BIC = Bayesian information criterion, SABIC = sample-adjusted Bayesian information criterion, BLRT = bootstrap likelihood ratio test.

MDLC scores for each digital readout were compared across baseline navigation profiles using linear models. Estimated marginal means and pairwise contrasts were computed to assess profile-specific differences.

ADRD biomarkers and navigation performance metrics

A multinomial logistic regression tested whether ADRD risk and reserve biomarkers, i.e., the age- and sex-adjusted MTL tau, EC thickness, hippocampal VD, PVS volumes in the centrum semiovale and basal ganglia, and WMH volume predicted baseline navigation profiles. Statistical interference for individual predictors was based on Wald z-tests of the coefficients, with two-sided p-values computed from the ratio of the estimated coefficients to their standard errors. To evaluate the unique contribution of each biomarker, full and reduced models were compared using likelihood ratio tests, and backward AIC-based model selection was performed to identify the most parsimonious predictive model.

To examine whether structural and vascular reserve markers modify the relationship between MTL tau burden and navigational efficiency, quantified by the path deviation MDLC score, we initially specified a linear regression model with path deviation MDLC score as the outcome and a three-way interaction between MTL tau burden, EC thickness, and hippocampal VD. Model simplification was then performed using backward elimination based on AIC and nested ANOVAs. This procedure indicated that the model retaining two two-way interaction terms (MTL tau × EC thickness and MTL tau × hippocampal VD, Supplementary Table 4) provided a better fit than the baseline model or a full three-way interaction model. We further conducted separate linear regression analyses using the number of map views and number of orientations stops MDLC scores as outcomes and centrum semiovale and basal ganglia PVS, as well as WMH as predictors to determine whether cerebrovascular disease markers impact learning on digital readouts capturing aspects of information processing and executive function (Supplementary Table 5 – 7).

Acknowledgements

This work was funded by the Deutsche Forschungsgemeinschaft (DFG (German Research Foundation) – Project-ID 425899996 – SFB 1436, and Project-ID 501214112). Computational PVS quantification was supported by The Galen and Hilary Weston Foundation under the Novel Biomarkers 2019 scheme (ref UB190097) administered by the Weston Brain Institute and the Row Fogo Charitable Trust (ref no. BRO-D. FID3668413). The funders had no role in study design, data collection and analysis, decision to publish, or preparation of the manuscript. We thank Jan Schlosshauer and his team at Intenta GmbH for the great cooperation and the realization of the "ExploreTrain" app and Christian Bobzien for the development of the 3D virtual environment of the medical campus Magdeburg. We further thank Sofia Laiker, Rebecca Schiemann, Clara Schwarz, Joseph Höpker-Fernandez, and Michèlle Maller for their assistance with data collection, and Canan Nazarov for conducting quality control of the T2-weighted images used in this study. Finally, we thank all study participants for their time and engagement, which made this research possible.

Author contributions

Conceptualization, J.M., A.M., and N.D.; Project administration, J.M., A.M., and N.D.; Investigation, J.M.; Methodology & Formal Analysis, J.M., N.V., N.B., B.S.-W., J.B., H.M., and A.M.; Data Curation, J.M., N.V., N.B., B.S.-W.; Resources, N.B., B.S.-W., A.H., A.-T.B., E. N. M., Sv.S., L.F., E.I.I., B.G.G., A.S., A.W.S., H.B., O.S., and E.D.; Visualization, J.M. and N.D.; Writing – Original Draft, J.M.; Writing – Review & Editing, A.M., and N.D.; Supervision, A.M. and N.D.; Funding Acquisition, St.S., E.K., E.D., H.B., M.K., A.M., and N.D.

Competing interests

ND is a full-time employee of neotiv GmbH. ED is Co-founder and Chief Medical Officer of neotiv GmbH. AWS is a full-time employer of Life Molecular Imaging GmbH. The remaining authors declare no competing interests.

Data availability

The datasets analyzed in this study may be made available on reasonable request from the corresponding author based on individual data transfer agreements.

Code availability

The underlying code for this study can be shared with qualified researchers on reasonable request from the corresponding author.

References

1. Nichols, E. *et al.* Estimation of the global prevalence of dementia in 2019 and forecasted prevalence in 2050: an analysis for the Global Burden of Disease Study 2019. *Lancet Public Health* **7**, e105–e125 (2022).

2. Livingston, G. *et al.* Dementia prevention, intervention, and care: 2020 report of the Lancet Commission. *The Lancet* **396**, 413 (2020).

3. Baker, L. *et al.* Structured vs self-guided multidomain lifestyle interventions for global cognitive function: The US POINTER randomized clinical trial. *JAMA* **334**, 681-691 (2025).

4. Silva, A. F. *et al.* Cognitive Training with Older Adults Using Smartphone and Web-Based Applications: A Scoping Review. *J. Prev. Alzheimers Dis.* **11**, 693–700 (2024).

5. Kourtis, L. C., Regele, O. B., Wright, J. M. & Jones, G. B. Digital biomarkers for Alzheimer's disease: the mobile/wearable devices opportunity. *Npj Digit. Med.* **2**, 1–9 (2019).

6. Polk, S. E. *et al.* A scoping review of remote and unsupervised digital cognitive assessments in preclinical Alzheimer's disease. *Npj Digit. Med.* **8**, 1–14 (2025).

7. Jutten, R. J. *et al.* Detecting early cognitive deficits in preclinical Alzheimer's disease using a remote digital multi-day learning paradigm. *Npj Digit. Med.* **8**, 1–10 (2025).

8. Jutten, R. J. *et al.* Lower practice effects as a marker of cognitive performance and dementia risk: A literature review. *Alzheimers Dement. Amst. Neth.* **12**, e12055 (2020).

9. Coughlan, G., Laczó, J., Hort, J., Minihane, A.-M. & Hornberger, M. Spatial navigation deficits — overlooked cognitive marker for preclinical Alzheimer disease? *Nat. Rev. Neurol.* **14**, 496–506 (2018).

10. Fricke, M. *et al.* Successful wayfinding in age: A scoping review on spatial navigation training in healthy older adults. *Front. Psychol.* **13**, (2022).

11. Lövdén, M. *et al.* Spatial navigation training protects the hippocampus against age-related changes during early and late adulthood. *Neurobiol. Aging* **33**, 620.e9-620.e22 (2012).

12. Yau, W.-Y. W. *et al.* Physical activity as a modifiable risk factor in preclinical Alzheimer's disease. *Nat. Med.* 1–9 (2025).

795 13. Marquardt, J. *et al.* Identifying older adults at risk for dementia based on smartphone data
796 obtained during a wayfinding task in the real world. *PLOS Digit. Health* **3**, e0000613 (2024).

797 14. Yushkevich, P. A. *et al.* Morphometry of medial temporal lobe subregions using high-
798 resolution T2-weighted MRI in ADNI3: Why, how, and what's next? *Alzheimers Dement.* **20**,
799 8113–8128 (2024).

800 15. Jack, C. R. & Holtzman, D. M. Biomarker Modeling of Alzheimer's Disease. *Neuron* **80**,
801 1347–1358 (2013).

802 16. Garcia-Garcia, B. *et al.* Vessel distance mapping: A novel methodology for assessing
803 vascular-induced cognitive resilience. *NeuroImage* **274**, 120094 (2023).

804 17. Düzel, E. & Bernal, J. Advances in imaging. In *Advances in the Management of Early*
805 *Alzheimer's Disease: Biological and Technological Advances* (ed. Chan, D.) 123–148 (Academic
806 Press, 2025).

807 18. Shaw, K. *et al.* Neurovascular coupling and oxygenation are decreased in hippocampus
808 compared to neocortex because of microvascular differences. *Nat. Commun.* **12**, 3190 (2021).

809 19. Prins, N. D. *et al.* Cerebral small-vessel disease and decline in information processing
810 speed, executive function and memory. *Brain* **128**, 2034–2041 (2005).

811 20. Veldsman, M. *et al.* Cerebrovascular risk factors impact frontoparietal network integrity
812 and executive function in healthy ageing. *Nat. Commun.* **11**, 4340 (2020).

813 21. van Dijk, E. J. *et al.* Progression of Cerebral Small Vessel Disease in Relation to Risk
814 Factors and Cognitive Consequences. *Stroke* **39**, 2712–2719 (2008).

815 22. Hamilton, O. K. L. *et al.* Cerebral small vessel disease burden and longitudinal cognitive
816 decline from age 73 to 82: the Lothian Birth Cohort 1936. *Transl. Psychiatry* **11**, 376 (2021).

817 23. Weizenbaum, E. L. *et al.* Capturing learning curves with the multiday Boston Remote
818 Assessment of Neurocognitive Health (BRANCH): Feasibility, reliability, and validity.
819 *Neuropsychology* **38**, 198–210 (2024).

820 24. Schellig, D., Günther, T., Schächtele, B. & Schuri, U. VWLT - Visueller Wege-Lerntest.
821 (2014).

822 25. Behrenbruch, N. *et al.* A physically and mentally active lifestyle relates to younger brain

823 and cognitive age. *GeroScience* **48**, 1853–1873 (2025).

824 26. Welsh, K. A. *et al.* The Consortium to Establish a Registry for Alzheimer's Disease
825 (CERAD). Part V. A normative study of the neuropsychological battery. *Neurology* **44**, 609–614
826 (1994).

827 27. Diersch, N., Valdes-Herrera, J. P., Tempelmann, C. & Wolbers, T. Increased Hippocampal
828 Excitability and Altered Learning Dynamics Mediate Cognitive Mapping Deficits in Human
829 Aging. *J. Neurosci.* **41**, 3204–3221 (2021).

830 28. Zhang, H., Zherdeva, K. & Ekstrom, A. D. Different "routes" to a cognitive map:
831 dissociable forms of spatial knowledge derived from route and cartographic map learning. *Mem.*
832 *Cognit.* **42**, 1106–1117 (2014).

833 29. Epstein, R. A., Patai, E. Z., Julian, J. B. & Spiers, H. J. The cognitive map in humans: spatial
834 navigation and beyond. *Nat. Neurosci.* **20**, 1504–1513 (2017).

835 30. Gardony, A. L., Taylor, H. A. & Brunyé, T. T. Gardony Map Drawing Analyzer: Software
836 for quantitative analysis of sketch maps. *Behav. Res. Methods* **48**, 151–177 (2016).

837 31. Berlin, K. S., Williams, N. A. & Parra, G. R. An Introduction to Latent Variable Mixture
838 Modeling (Part 1): Overview and Cross-Sectional Latent Class and Latent Profile Analyses. *J.*
839 *Pediatr. Psychol.* **39**, 174–187 (2014).

840 32. Caselli, R. J. *et al.* The neuropsychology of normal aging and preclinical Alzheimer's
841 disease. *Alzheimers Dement.* **10**, 84–92 (2014).

842 33. Stern, Y. *et al.* A framework for concepts of reserve and resilience in aging. *Neurobiol.*
843 *Aging* **124**, 100–103 (2023).

844 34. Hassenstab, J. *et al.* Absence of practice effects in preclinical Alzheimer's disease.
845 *Neuropsychology* **29**, 940–948 (2015).

846 35. Samaroo, A. *et al.* Diminished Learning Over Repeated Exposures (LORE) in preclinical
847 Alzheimer's disease. *Alzheimers Dement.* **12**, e12132 (2020).

848 36. Öhman, F., Hassenstab, J., Berron, D., Schöll, M. & Papp, K. V. Current advances in digital
849 cognitive assessment for preclinical Alzheimer's disease. *Alzheimers Dement. Diagn. Assess. Dis.*
850 *Monit.* **13**, e12217 (2021).

37. Lee, H. *et al.* Aberrant vascular architecture in the hippocampus correlates with tau burden in mild cognitive impairment and Alzheimer's disease. *J. Cereb. Blood Flow Metab.* **44**, 787–800 (2024).

38. Schreiber, S. & DiFrancesco, J. C. Impaired occipital cerebrovascular reactivity as a biomarker for vascular β-amyloid. *Neurology* **95**, 415–416 (2020).

39. Mitolo, M., Borella ,Erika, Meneghetti ,Chiara, Carbone ,Elena & and Pazzaglia, F. How to enhance route learning and visuo-spatial working memory in aging: a training for residential care home residents. *Aging Ment. Health* **21**, 562–570 (2017).

40. Vermeir, J. F., White, M. J., Johnson, D., Crombez, G. & Ryckeghem, D. M. L. V. The Effects of Gamification on Computerized Cognitive Training: Systematic Review and Meta-Analysis. *JMIR Serious Games* **8**, e18644 (2020).

41. Wilson, R. S. *et al.* Participation in Cognitively Stimulating Activities and Risk of Incident Alzheimer Disease. *JAMA* **287**, 742–748 (2002).

42. Thomas, K. R. *et al.* Cognitive Heterogeneity and Risk of Progression in Data-Driven Subtle Cognitive Decline Phenotypes. *J. Alzheimer's Dis.* **90**, 323–331 (2022).

43. Jak, A. J. *et al.* Quantification of Five Neuropsychological Approaches to Defining Mild Cognitive Impairment. *Am. J. Geriatr. Psychiatry* **17**, 368–375 (2009).

44. Lillig, R. *et al.* A new CERAD total score with equally weighted *z*-scores and additional executive and non-amnestic „CERAD-Plus" tests enhances cognitive diagnosis in patients with Parkinson's disease: Evidence from the LANDSCAPE study. *Parkinsonism Relat. Disord.* **90**, 90–97 (2021).

45. Mattern, H. *et al.* Prospective motion correction enables highest resolution time-of-flight angiography at 7T. *Magn. Reson. Med.* **80**, 248–258 (2018).

46. Menze, I. *et al.* Perivascular space enlargement accelerates in ageing and Alzheimer's disease pathology: evidence from a three-year longitudinal multicentre study. *Alzheimers Res. Ther.* **16**, 242 (2024).

47. Valdés Hernández, M. del C. *et al.* Influence of threshold selection and image sequence in in-vivo segmentation of enlarged perivascular spaces. *J. Neurosci. Methods* **403**, 110037 (2024).

879 48. Potter, G. M., Chappell, F. M., Morris, Z. & Wardlaw, J. M. Cerebral Perivascular Spaces
880 Visible on Magnetic Resonance Imaging: Development of a Qualitative Rating Scale and its
881 Observer Reliability. *Cerebrovasc. Dis.* **39**, 224–231 (2015).

882 49. Peterson, R. Finding Optimal Normalizing Transformations via bestNormalize. *R J.*
883 https://digitalcommons.unl.edu/r-journal/17 (2021).

884 50. Wiltgen, T. *et al.* LST-AI: A deep learning ensemble for accurate MS lesion segmentation.
885 *NeuroImage Clin.* **42**, 103611 (2024).

886 51. Joshi, A. A., Shattuck, D. W. & Leahy, R. M. A Method for Automated Cortical Surface
887 Registration and Labeling. In *Biomedical Image Registration* (eds. Dawant, B. M., Christensen, G.
888 E., Fitzpatrick, J. M. & Rueckert, D.) 180–189 (Springer, 2012).

889 52. Yushkevich, P. A. *et al.* Automated volumetry and regional thickness analysis of
890 hippocampal subfields and medial temporal cortical structures in mild cognitive impairment.
891 *Hum. Brain Mapp.* **36**, 258–287 (2015).

892 53. Mattern, H. Openly available sMall vEsseL sEgmenTaTion pipelinE (OMELETTE).).In:
893 Poster presented at 29th Annual Meeting of International Society of Magnetic Resonance in
894 Medicine (ISMRM), 15–20 (2021).

895 54. Rullmann, M. *et al.* A multicenter [18F]PI-2620 PET study for in vivo staging of tau
896 pathology in progressive supranuclear palsy. *J. Nucl. Med.* **63**, 2224–2224 (2022).

897 55. Brendel, M. *et al.* Assessment of 18F-PI-2620 as a Biomarker in Progressive Supranuclear
898 Palsy. *JAMA Neurol.* **77**, 1408–1419 (2020).

899 56. Bates, D., Mächler, M., Bolker, B. & Walker, S. Fitting Linear Mixed-Effects Models using
900 lme4. J. Stat. Softw. 67, 1–48 (2015).

901 57. Brooks, M. E. *et al.* glmmTMB balances speed and flexibility among packages for zero-
902 inflated generalized linear mixed modeling. *R J.* **9**, 378–400 (2017).

903

Supplementary Files

This is a list of supplementary files associated with this preprint. Click to download.

- SITable1.docx
- SITable2.docx
- SITable3.docx
- SITable4.docx
- SITable5.docx
- SITable6.docx
- SITable7.docx
- SITable8.docx
- MobilewayfindingtrainingandlearningtrajectoriesMarquardtetal2026SI.docx
- SIFigure1MDLC.tiff
- SIFigure2MDLCProfiles.tiff
- SIFigure3LandmarkRecognition.tiff
- SIFigure4MapDrawing.tiff
- SIFigure5MovementTrajectories.tiff